protein structure communications

Structure of human salivary α-amylase crystallized in a C-centered monoclinic space group

S. Zoë Fisher,[a] Lakshmanan Govindasamy,[a] Chingkuang Tu,[b] Mavis Agbandje-McKenna,[a] David N. Silverman,[b] Hannu J. Rajaniemi[c] and Robert McKenna[a]*

[a]Department of Biochemistry and Molecular Biology, University of Florida, Gainesville, FL 32601, USA, [b]Department of Pharmacology and Therapeutics, University of Florida, Gainesville, FL 32601, USA, and [c]Department of Anatomy and Cell Biology, PO Box 5000, University of Oulu, Oulu, Finland

Correspondence e-mail: rmckenna@ufl.edu

Human salivary α-amylase (HSA) is a major secretory protein component of saliva and has important biological functions, including the initial digestion of starch. HSA acts as a monomer and mediates the hydrolysis of α-1,4-glucosidic linkages in oligosaccharides. To date, all published crystal structures of HSA have been crystallized as monomers in space group $P2_12_12_1$. Here, the serendipitous purification, crystallization and ultimate structure determination of a HSA non-crystallographic symmetry (NCS) dimer, while attempting to purify human carbonic anhydrase VI (HCA VI) from saliva using an affinity resin for α-class carbonic anhydrases, is presented. On further investigation, it was shown that HSA could only be copurified using the affinity resin in the presence of HCA VI which is glycosylated and not the non-glycosylated HCA II. The identification of the HSA crystals was carried out by peptide mapping and mass spectrometry. HSA was shown to have crystallized as an NCS dimer in space group $C2$, with unit-cell parameters $a = 150.9$, $b = 72.3$, $c = 91.3$ Å, $\beta = 102.8°$. The NCS dimer crystal structure is reported to 3.0 Å resolution, with a refined R_{cryst} of 0.228. The structure is compared with the previously reported $P2_12_12_1$ monomer structures and the crystal packing and dimer interface are discussed.

1. Introduction

The hydrolases and transferases that belong to the α-amylase family are endoglycosidases and are found across species, from plants to humans (Janeček, 1997). Human α-amylase (HSA) is a secretory protein that is produced by both the pancreas and salivary glands. Clinically, HSA has been studied extensively because abberant secretion and activity of this enzyme can be used to detect abnormalities in the organs of origin (Kandra & Gyémánt, 2000). Human salivary α-amylase (HSA; α-1,4-D-glucan glucanohydrolase; EC 3.2.1.1) constitutes a significant proportion of saliva and plays an important digestive role in the initial digestion of starch, glycogen and other polysaccharides. It acts as a monomer and catalyzes the hydrolysis of α-1,4-glucosidic linkages, yielding oligosaccharide in the α-anomeric configuration (Ramasubbu et al., 1996; MacGregor et al., 2001).

HSA consists of 496 amino acids and is found in two forms in human saliva: a glycosylated isoform (apparent molecular weight 62 kDa) and a non-glycosylated form of 56 kDa (Bank et al., 1991). Recent subsite-mapping studies indicate the active-site cleft as having seven substrate subsites, with negative numbering extending to the site where the non-reducing end of the oligosaccharide resides and positive numbers for the reducing end. The oligosaccharide binds in the cleft with one monomer per subsite and the scissile bond is then cleaved by catalytic residues located between sites (+1) and (−1) (Ramasubbu et al., 1996; Kandra et al., 2003).

The α-amylases are multidomain proteins that display low overall sequence identity and different substrate specificities. These enzymes have a variable number of domains, but the common motif is a $(\beta/\alpha)_8$-barrel that contains the active site/catalytic core (MacGregor et al., 2001).

The HSA structure consists of three domains (A, B and C): domain A (residues 1–99 and 169–404) contains the common amylase $(\beta/\alpha)_8$-barrel motif, domain B (residues 100–168) consists of an open
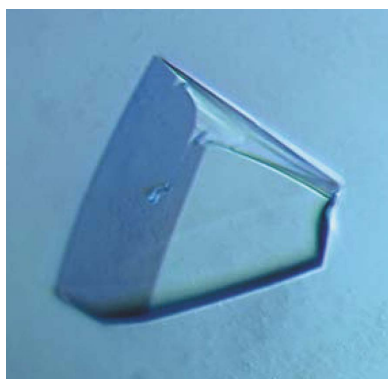
loop that contains several helices and β-strands and domain C (residues 405–496) is composed of ten β-strands of which eight form a Greek-key motif. The catalytic residues (Asp197, Glu233 and Asp300) are found in domain A and are in close proximity to each other in the substrate-binding cleft and surround the proposed (+1) and (−1) interface region (Ramasubbu et al., 1996). HSA binds a chloride ion near the active site in domain A and is coordinated by the side chains of Arg195, Asn298 and Arg337 and a calcium ion that is coordinated by His201 from domain A and Asn100, Arg158 and Asp167 from domain B. The exact function of domain C remains unclear, but it has been postulated to play a role in the stabilization of domain A as it seems to shield hydrophobic residues from bulk solvent (MacGregor et al., 2001). More than 30 crystal structures of α-amylase (including recombinant and wild-type human pancreatic and salivary and porcine) have been reported in the orthorhombic system (e.g. PDB codes 1jxj, 1jxk and 1kbb; Rydberg et al., 2002; Ramasubbu et al., 2003). We have crystallized HSA in the monoclinic space group $C2$ with two molecules in the asymmetric unit. The $C2$ HSA non-crystallographic symmetry (NCS) dimer crystal packing is compared with previously solved $P2_12_12_1$ HSA monomer structures and the NCS dimer interface, contacts and buried surfaces are discussed.

2. Materials and methods

2.1. Sample preparation from human saliva

Human saliva collection was performed as described previously (Kivela et al., 2003). Briefly, saliva secretion was stimulated by chewing paraffin wax and saliva was then collected by spitting into test tubes that were kept on ice. After collection, the samples were frozen and stored at 253 K. Thawed whole saliva samples were centrifuged at 15 000g for 10 min at 277 K and the supernatant was diluted fourfold with buffer (0.1 M Tris–SO$_4$, 0.2 M Na$_2$SO$_4$ pH 8.7 and 1 mM benzamidine). The sample was loaded onto p-amino-benzenesulfonamide (pAMBS) coupled to Sepharose beads (an affinity resin commonly used to purify α-class carbonic anhydrases; Khalifah et al., 1977) and the unbound material was washed off with 20 column volumes buffer (0.1 M Tris–HCl, 0.2 M Na$_2$SO$_4$ pH 9.0). To further remove non-specifically bound material, the pH was changed to 7.0 and washing continued until the OD$_{280}$ reached zero. Bound protein was eluted with 0.1 M Tris–SO$_4$, 0.4 M NaN$_3$, 1 mM benzamidine pH 8.7 and fractions containing protein were pooled, buffer-exchanged using a Hi-Trap Desalting column (Pharmacia) into 50 mM Tris–HCl pH 7.5 and concentrated to ~10 mg ml^{-1}.

A silver-stained gel (8–25% SDS–PAGE) of eluted fractions from the pAMBS column showed the presence of two bands (see supplementary material[1]): a 42 kDa protein, the expected HCA VI, and a 56 kDa protein, later identified as HSA (see §2.2).

2.2. MALDI–TOF MS and HSA identification

In order to identify the 56 kDa protein, the band was excised from the SDS–PAGE gel for MALDI–TOF (Matrix Assisted Laser-Desorption Ionization Time-of-Flight) mass-spectrometry analysis. An in-gel tryptic digest was performed as described previously (Shevchenko et al., 1996) and the resulting peptides were mixed with the matrix (α-cyano-4-hydroxycinnamic acid) in a 1:1 ratio and spotted onto a MALDI–TOF sample plate. Peptide masses were obtained using an in-house PerSeptive Biosystems Voyager MALDI–

TOF mass spectrometer. The resulting peptide masses were searched against the database using the ProteinProspector database (http://prospector.ucsf.edu) and the higher molecular-weight protein was identified as HSA.

2.3. Copurification of HSA and HCA VI

To test for non-specific binding of HSA to the pAMBS column, pure HSA was purchased (Sigma) and reconstituted as per the manufacturer's instructions to ~1 mg ml^{-1}. This was the loaded onto the pAMBS column (as described in §2.1) and the flowthrough (unbound material), wash and elution fractions were collected and run on a 12% SDS–PAGE gel (Fig. 1a). To rule out a non-specific protein–protein interaction between carbonic anhydrases and HSA, an approximately fivefold excess of human carbonic anhydrase II (HCA II), a non-glycosylated carbonic anhydrase, and HSA were mixed and allowed to incubate at 277 K for 4 h. The mixed proteins were then subjected to affinity chromatography as described for the HSA alone (Fig. 1b). Finally, a similar experiment was performed with equal amounts of HCA VI and HSA (Fig. 1c).

2.4. Crystallization of HSA

Initial crystallization screens were conducted with Hampton Research Crystal Screens 1 and 2 using the hanging-drop vapor-diffusion method (McPherson, 1982) on the purified sample containing both HCA VI and HSA (at the time unknown 56 kDa) proteins (see supplementary material[1]). Crystal drops were prepared by mixing 1 µl 10 mg ml^{-1} protein solution (in 50 mM Tris–HCl pH 7.5) and 1 µl precipitant solution. The drops were equilibrated by vapor diffusion against 0.4 ml precipitant solution at 277 K.

Three of the screening conditions yielded promising crystals within one week of crystallization set-up: (i) 0.2 M magnesium acetate tetrahydrate, 0.1 M sodium cacodylate pH 6.5, 20%(w/v) poly-ethylene glycol 8000 (Crystal Screen 1 condition No. 18), (ii) 0.2 M
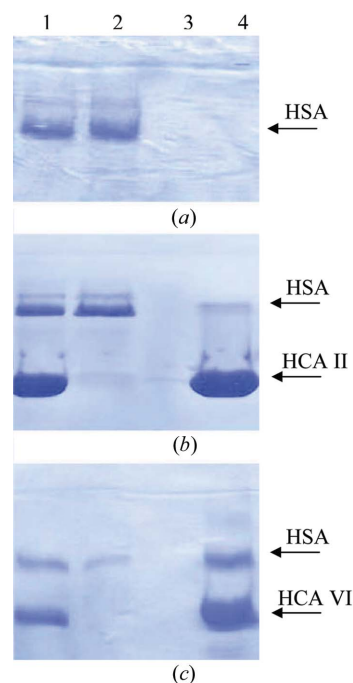
Figure 1
Coomassie-stained SDS–PAGE gels. (a) HSA alone, (b) HSA and HCA II and (c) HSA and HCA VI. Lane 1, load/input onto pAMBS column; lane 2, flowthrough/unbound material; lane 3, wash fraction; lane 4, eluted fraction.

Table 1
Data-collection and refinement statistics.

Values for the highest resolution shell are given in parentheses.

Space group	$C2$
Unit-cell parameters (Å, °)	$a = 150.9$, $b = 72.3$, $c = 91.3$, $\beta = 102.8$
V_M (Å³ Da⁻¹)	2.2
Calculated solvent content (%)	40.9
Resolution range (Å)	20.0–3.0 (3.11–3.00)
Total observed reflections	38453
Unique reflections/redundancy	18581/2.1
$I/\sigma(I)$	3.1 (2.5)
Completeness (%)	96.2 (95.6)
R_{sym}† (%)	16.6 (33.1)
R_{cryst}/R_{free}‡ (%)	22.8/27.1
No. of protein/solvent/ion atoms	3945/65/2
R.m.s.d.§ bond lengths (Å)/angles (°)	0.007/1.4
Average B factor protein atoms (Å²)	20.4
Average B factor solvent/ions (Å²)	25.6/14.4
Dimer buried surface area (Å²)	∼2800
Ramachandran statistics¶ (%)	
Most favored	81.2
Additionally allowed	18.8

† $R_{sym} = \sum |I - \langle I \rangle| / \sum I$, where I is the intensity of a reflection and $\langle I \rangle$ is the average intensity. ‡ $R_{cryst} = \sum_{hkl} |F_o - F_c| / \sum_{hkl} |F_o|$; R_{free} is calculated from 5% of data for cross-validation. § R.m.s.d., root-mean-square deviation. ¶ Ramachandran & Sasisekharan (1968).

calcium acetate, 0.1 M sodium cacodylate pH 6.5, 18%(w/v) polyethylene glycol 8000 (Crystal Screen 1 condition No. 46) and (iii) 0.1 M MES pH 6.5, 12%(w/v) polyethylene glycol 20 000 (Crystal Screen 2 condition No. 22).

After testing the X-ray diffraction quality of crystals from all three conditions, only crystals (Fig. 2) from condition (ii) showed suitable ordered diffraction for structural studies.

2.5. Data collection of HSA

Data were collected using an R-AXIS IV⁺⁺ image-plate system equipped with Osmic mirrors and a Rigaku HU-H3R CU rotating-anode generator operating at 50 kV and 100 mA. A 0.3 mm collimator was used with a crystal-to-detector distance of 120 mm and the 2θ angle fixed at 0°. A single crystal was briefly dipped into a cryoprotectant (30% glycerol mixed with precipitant solution), placed on a thin nylon crystal-mounting loop (Hampton Research) and flash-frozen in a liquid nitrogen-gas stream (Oxford Cryosystems). All diffraction data frames were collected using a 1.0° oscillation angle with an exposure time of 300 s per frame at 100 K. The data set was indexed using *DENZO* (see supplementary material) and scaled and reduced with *SCALEPACK* software (Otwinowski & Minor, 1997). The Bragg reflection amplitudes for all the data were converted into structure factors using *TRUNCATE* (Collaborative Computational Project, Number 4, 1994). Data-collection statistics are given in the supplementary material.

### 2.6. Structure determination and refinement of HSA dimer

The HSA structure was solved using the molecular-replacement method (Rossmann, 1990). A monomer of HSA (PDB code 1jxj; Ramasubbu *et al.*, 2003) with ions and solvent molecules removed was used as the search model for cross-rotation function and translation searches for two molecules using the program *MOLREP* (Vagin & Teplyakov, 1997). After initial rigid-body refinement, the NCS operator was determined by least-squares fit of the two independently assigned HSA monomers and applied to all subsequent refinement using the *CNS* program suite (Brünger *et al.*, 1998). Further model refinement was carried out using simulated annealing and iterative rounds of individual B-factor refinement and energy

minimization. Examination of the initial $|F_o - F_c|$ and $2|F_o - F_c|$ electron-density maps clearly identified the N-terminal pyroglutamic acid, Ca^{2+} and Cl^- ions, which were subsequently manually built using the molecular-graphics program *O* v.7 (Jones, 1978). The reliability of the model was checked by omitting 20 amino acids at a time from the model and rebuilding into the resultant calculated $|F_o - F_c|$ electron-density maps. After several cycles of standard refinement methods (refining both position and thermal parameters) and manual rebuilding, solvent molecules were added (using a 3σ cutoff) using the automated water-picking program in *CNS*. The criteria for solvent selection and retention were that no solvent molecules were closer than 2.6 Å or further than 3.6 Å from any protein atoms and that with an assigned occupancy of 1.0 the final refined B value was no greater than 40.0 Å². Further refinement continued until R_{cryst} and R_{free} converged. A randomly assigned 5% of the observed reflections were omitted from refinement and used for R_{free} calculations. Data-collection and refinement statistics are given in Table 1. Buried surface-area calculations were performed using *CNS*.

3. Results and discussion

3.1. Copurification of HSA and HCA VI

The unexpected observation of copurification of HSA and HCA VI from saliva using the pAMBS column (see supplementary material) led us to investigate further the purification of HSA alone, mixed with HCA II and mixed with HCA VI using the carbonic anhydrase affinity column (Fig. 1). The results were that HSA alone does not bind the affinity column, as all the HSA was observed in the flowthrough fraction (Fig. 1a), that there does not appear to be a significant interaction between HCA II (a non-glycosylated carbonic anhydrase) and HSA, as the bulk of HSA appears in the unbound fraction while all the HCA II stays bound to the column (Fig. 1b), but that HSA in the presence of HCA IV does bind to the column with only a small amount of unbound HSA in the flowthrough fraction (Fig. 1c). These results imply that HCA VI and HSA have some affinity for each other in saliva and/or in solution and that this interaction is possibly because HCA IV is glycosylated (Feldstein & Silverman, 1982; Thatcher *et al.*, 1998).
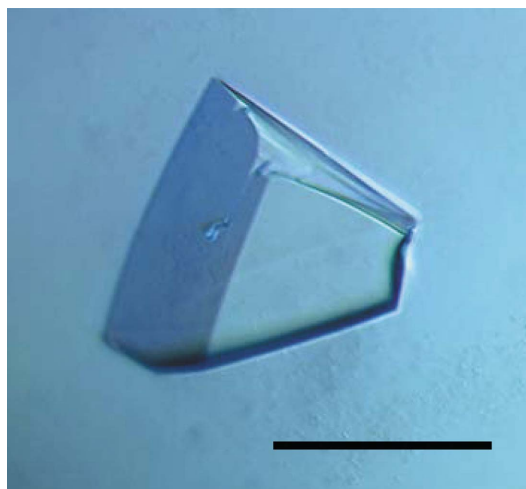
Figure 2
Optical photograph of HSA crystal. The bar indicates 0.1 mm. This photograph was taken with a Bio-Rad 1024 ES confocal microscope with an Olympus IX 70 transmission.

3.2. Crystallization of HSA

Another unexpected result was the successful crystallization of solely HSA (Fig. 2) from the mixture of HSA and HCA VI, as HCA VI was effectively an impurity in the crystallization setup (condition ii). Under these circumstances, a complex of both enzymes might usually be expected as the possible outcome if crystal growth is observed. It may be worth pursuing other crystallization conditions to see whether such a complex can be crystallized. There are some reports that indicate that HSA and HCA VI could have a biological interaction in that both enzymes follow the same circadian expression pattern in humans (Parkkila *et al.*, 1995). Also, immunostaining experiments of the human enamel pellicle formed *in vivo* also show that both HSA and HCA VI display similar patterns of staining (Leinonen *et al.*, 1999). Another interesting study in rat parotid cells showed that the absence of bicarbonate caused a 50% reduction in the secretion of HSA (Youssef *et al.*, 2003). Whether the above circumstantial evidence indicates a physiological significance of a complex between HSA and HCA VI is still unclear.

3.3. Structure determination of HSA

A total of 100° of data were collected from a single HSA crystal that diffracted to a maximum useful resolution of 3.0 Å. Inspection of the *DENZO* (Otwinowski & Minor, 1997) output, listing the 14 possible Bravais lattices and percentage distortion index (see supplementary material), clearly indicated that the HSA had crystallized as *C*-centered monoclinic (0.14%) and not primitive ortho-rhombic (12.64%); thus, the data were therefore assigned to space group *C*2 (see supplementary material and Table 1).

From the unit-cell volume and the molecular weight of HSA, a V_M value (Matthews, 1968) of 2.2 $\mathring{A}^3\,Da^{-1}$ was calculated for two molecules per asymmetric unit (with a solvent fraction of 40.9% assuming a partial specific volume of 0.74 $cm^3\,g^{-1}$) using *CNS* v.1.1 (Brünger *et al.*, 1998). This result indicating the HSA had crystallized as an NCS dimer.

A cross-rotation function, using a previously determined HSA monomer (PDB code 1jxj; Ramasubbu *et al.*, 2003), resulted in two clear solutions, *A* (α = 349.9, β = 0.0, γ = 9.9°) and *B* (α = 112.7, β = 44.3, γ = 65.7°), with peak heights of 20.4 and 17.6σ above the mean, respectively. A translation-function calculation using the cross-rotation function results placed solution *A* at T_x = 0.468, T_y = 0.000, T_z = 0.258 (fractional coordinates) and solution *B* at T_x = 0.231, T_y = 0.000, T_z = 0.267. The combined R_{work} for the two HSA monomers in the crystallographic asymmetric unit was 0.344, with a correlation coefficient of 0.634. After one round of rigid-body refinement of with two independent HSA monomers (R_{work} and R_{free} were reduced to 0.303 and 0.305, respectively), the NCS operator was determined and applied to all subsequent cycles of refinement on the solution *A* monomer.

3.4. Structure of HSA

The final refined structure of HSA consists of 3945 atoms (496 residues), including the N-terminal pyroglutamic acid, one Ca^{2+} ion, one Cl^- ion and 65 solvent molecules. The reliable placement of plausible solvent molecules was limited by the 3.0 Å resolution of the data set.
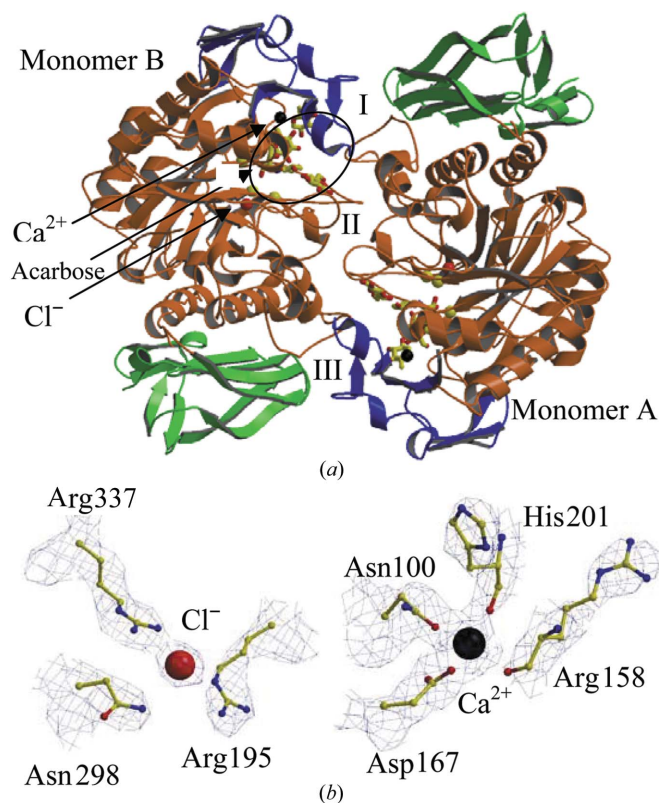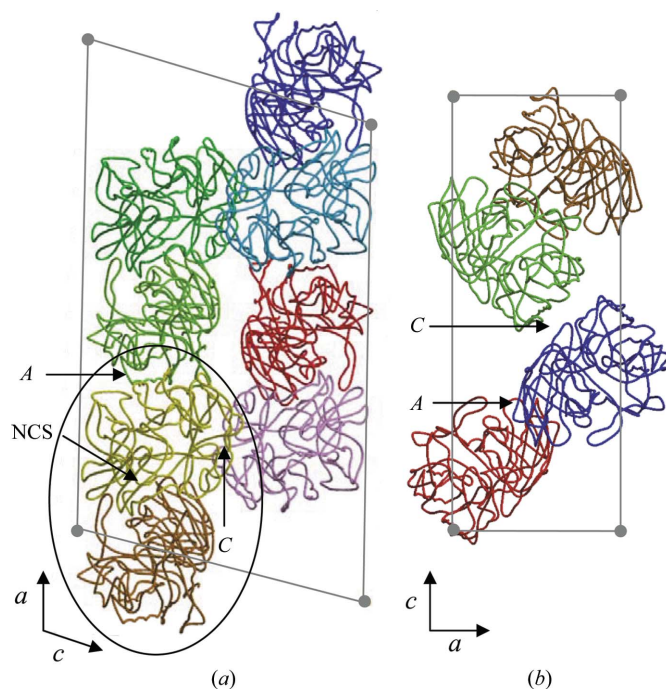

Figure 3
HSA dimer structure. (*a*) Ribbon diagram depicting the NCS dimer interface. Secondary-structure elements are as depicted; domains *A*, *B* and *C* are colored orange, blue and green, respectively, for each monomer, Cl^- and Ca^{2+} ions are depicted as a red and black spheres, respectively, active-site residues (Asp197, Glu233 and Asp300) are shown as yellow spheres and the inhibitor acarbose, shown in yellow ball-and-stick representation, was modeled into the active site of each dimer by least-squares fitting each monomer to a previously determined structure of HSA (PDB code 1b2y; Qian *et al.*, 1994). The labels I, II and III denote regions of monomer–monomer interdigitation. (*b*) Ball-and-stick diagram of residues involved in Cl^--ion (red sphere) coordination are shown and labeled. $2|F_o - F_c|$ density (blue) is shown contoured at 1.5σ for the Cl^- ion and at 1.2σ for the amino-acid side chains. The electron density shown is from this study. (*c*) Ball-and-stick diagram of residues involved in Ca^{2+}-ion (black sphere) coordination. The electron density is contoured at the same level as in (*b*). (*d*) Molecular-surface representation with charge distribution of the HSA dimer (rotated by 20 and 30° along the *x* and *y* axes, respectively, compared with the view in *a*). The black arrow indicates the location of the inihibitor acarbose in the active site of monomer *A*. (*a*)–(*c*) were generated with *BobScript* (Esnouf, 1999) and (*d*) with *GRASP* (Nicholls *et al.*, 1991).

Fig. 3(a) shows the overall topology and secondary-structure elements of HSA with domains A (orange), B (blue) and C (green). The quality of the final model was assessed using the program *PROCHECK* and was shown to be satisfactory (Laskowski *et al.*, 1993; see supplementary data and Table 1).

The ion-binding sites were similar to those observed in previously determined HSA monomer structures. The Cl^- ion located in domain A (red sphere in Figs. 3a and 3b) and is tricoordinated by the side chains of residues Arg195 (NE, 3.2 Å), Asn298 (ND2, 3.4 Å) and Arg337 (NH2, 3.1 Å) found near the active site and catalytic residues (Asp197, Glu233 and Asp300). The Ca^{2+} ion located at the interface between domains A and B (black sphere in Figs. 3a and 3c) and is pentacoordinated by the side chains of residues Asn100 (OD1, 2.3 Å), Asp167 (OD1, 3.2 Å; OD2, 2.7 Å) as well as the carbonyl O atom of residues Arg158 (2.3 Å) and His201 (2.2 Å). A previously reported solvent molecule that completes the Ca^{2+} ion coordination (Ramasubbu *et al.*, 1996) was not observed at 3.0 Å resolution.

3.5. HSA packing and dimer interface

The NCS dimer is observed to be an antiparallel dimer with domain A from each monomer contributing most to the interface. The interface is a complex interdigitation of loops between the monomers (Fig. 3a). This creates a large amount of buried surface area between the dimer interface (~2800 Å^2; Fig. 3d). This is significantly higher than the average amount of buried surface in biological systems, such as antigen–antibody and protease–inhibitor complexes, which have an average buried surface of 1600 (±400) Å^2 (Lo Conte *et al.*, 1999).

The monomer–monomer interactions can be broken down into three broad contact regions of interdigitating loops: (I) an extended loop region, residues 143–156 (domain B) of monomer A interacting with residues 270–286 (domain B) of monomer B, (II) residues 235–245 (domain A) of monomer A interacting with the corresponding residues of monomer B (of interest is the Gly238 and Gly239 contact point, which is located at the center of rotational symmetry between the two monomers) and (III) the converse of the interactions observed in region I (Fig. 3a). The interactions observed are mainly hydrophobic in nature, although it seems likely hydrogen-bonding interactions are plausible between the interface, but the lack of high-resolution data (only to 3.0 Å) makes it difficult to correctly assign more solvent molecules in this region. The HSA dimer reported here demonstrates little conformational change from previously reported monomer forms; for example, the monomer of PDB code 1jxj (Ramasubbu *et al.*, 2003) has an r.m.s.d. for C$^\alpha$ atoms of only 0.32 Å when compared with monomer A of the dimer.

In order to assess whether the antiparallel dimer could be functional, the HSA acarbose inhibitor monomer complex structure (PDB code 1b2y; Qian *et al.*, 1994) was least-squares fitted independently onto each monomer of the dimer. Both the fitted acarboses within their respective monomers were solvent-accessible and exhibited no steric clashes within the active sites of the monomers (Figs. 3a and 3d). Therefore, it is plausible that sugar moieties could bind in the HSA NCS dimer configuration as reported in this paper.

Fig. 4 highlights the difference in the packing arrangements and relative orientations of the HSA NCS dimers and monomers in the C2 and P2$_1$2$_1$2$_1$ space groups, respectively. As mentioned, the HSA NCS dimer buried surface area is ~2800 Å^2, whereas the crystal contacts within the lattice are significantly less; for example, along the a and c axes they are ~800 and ~1000 Å^2, respectively (Fig. 4a, contacts A and C). In comparison, the crystal contacts of the HSA monomers in the P2$_1$2$_1$2$_1$ space group, for example, are ~700 and ~1600 Å^2 along the a and c axes, respectively (Fig. 4b, contacts A and C). Additionally, in the C2 packing, the HSA NCS dimers lie approximately parallel to the a axis and this directional arrangement may contribute to the lower diffraction quality of the crystals (3.0 Å resolution) compared with the staggered array of the HSA monomers observed in the P2$_1$2$_1$2$_1$ packing that diffract significantly better to 2.0 Å resolution (PDB code 1jxj; Ramasubbu *et al.*, 2003).

In conclusion, it would appear that HSA has an affinity for the glycosylated HCA VI, but not the non-glycosylated HCA II, and therefore this interaction is most likely to be mediated by the oligosaccharide moiety attached to HCA VI. Also, we report the first observed plausible functional HSA dimer configuration; the active site of each monomer is solvent-accessible and therefore theoretically could be functional, although there is no biological evidence for HSA acting as a dimer in the current literature to date.

Figure 4

HSA ribbon packing in C2 and P2$_1$2$_1$2$_1$ crystal lattices. Crystal lattice packing diagrams viewed down the b axes of the (a) C2 (this study) and (b) P2$_1$2$_1$2$_1$ (PDB code 1jxj; Ramasubbu *et al.*, 2003) crystal forms of HSA, respectively. (a) The C2 packing arrangement of four antiparallel HSA dimers depicted as orange and yellow (highlighted by an open ellipsoid), green and light green, blue and cyan, and red and purple pairs. (b) The P2$_1$2$_1$2$_1$ packing arrangement of the four HSA monomers depicted in red, blue, green and orange. Arrows point to the NCS dimer interface and crystal contacts, marked NCS, A and C, respectively. The figure was generated with *BobScript* (Esnouf, 1999).

References

Bank, R. A., Hettema, E. H., Arwert, F., Amerongen, A. V. & Pronk, J. C. (1991). *Electrophoresis*, **12**, 74–79.

Brünger, A. T., Adams, P. D., Clore, G. M., DeLano, W. L., Gross, P., Grosse-Kunstleve, R. W., Jiang, J.-S., Kuszewski, J., Nilges, N., Pannu, N. S., Read, R. J., Rice, L. M., Simonson, T. & Warren, G. L. (1998). *Acta Cryst.* D**54**, 905–921.

Collaborative Computational Project, Number 4 (1994). *Acta Cryst.* D**50**, 760–763.

Esnouf, R. M. (1999). *Acta Cryst.* D**55**, 938–940.

Feldstein, J. B. & Silverman, D. N. (1982). *J. Biol. Chem.* **259**, 5447–5453.

Janeček, S. (1997). *Prog. Biophys. Mol. Biol.* **67**, 67–97.

Jones, T. A. (1978). *J. Appl. Cryst.* **11**, 268–272.

Kandra, L. & Gyémánt, G. (2000). *Carbohydr. Res.* **329**, 579–585.

Kandra, L., Gyémánt, G., Remenyik, J., Ragunath, C. & Ramasubbu, N. (2003). *FEBS Lett.* **544**, 194–198.

Khalifah, R. G., Strader, D. J., Bryant, S. H. & Gibson, S. M. (1977). *Biochemistry*, **16**, 2241–2247.

Kivela, J., Laine, M., Parkkila, S. & Rajaniemi, H. (2003). *Arch. Oral Biol.* **48**, 547–551.

Laskowski, R. A., MacArthur, M. W., Moss, D. S. & Thornton, J. M. (1993). *J. Appl. Cryst.* **26**, 283–291.

Leinonen, J., Kivela, J., Parkkila, S., Parkkila, A. K. & Rajaniemi, H. (1999). *Caries Res.* **33**, 185–190.

Lo Conte, L., Chothia, C. & Janin, J. (1999). *J. Mol. Biol.* **285**, 2177–2198.

MacGregor, E. A., Janeček, S. & Svensson, B. (2001). *Biochim. Biophys. Acta*, **1546**, 1–20.

McPherson, A. (1982). *Preparation and Analysis of Protein Crystals.* New York: Wiley & Sons.

Matthews, B. W. (1968). *J. Mol. Biol.* **33**, 491–497.

Nicholls, A., Sharp, K. & Honig, B. (1991). *Proteins*, **11**, 281–296.

Otwinowski, Z. & Minor, W. (1997). *Methods Enzymol.* **276**, 307–326.

Parkkila, S., Parkkila, A. K. & Rajaniemi, H. (1995). *Acta Physiol. Scand.* **154**, 205–211.

Qian, M., Haser, R., Buisson, G., Duee, E. & Payan, F. (1994). *Biochemistry*, **33**, 6284–6294.

Ramachandran, G. N. & Sasisekharan, V. (1968). *Adv. Protein Chem.* **23**, 283–438.

Ramasubbu, N., Paloth, V., Luo, Y., Brayer, G. D. & Levine, M. J. (1996). *Acta Cryst.* D**52**, 435–446.

Ramasubbu, N., Ragunath, C. & Mishra, P. J. (2003). *J. Mol. Biol.* **325**, 1061–1076.

Rossmann, M. G. (1990). *Acta Cryst.* A**46**, 73–82.

Rydberg, E. H., Li, C., Maurus, R., Overall, C. M., Brayer, G. D. & Withers, S. G. (2002). *Biochemistry*, **41**, 4492–4502.

Shevchenko, A., Wilm, M., Vorm, O. & Mann, M. (1996). *Anal. Chem.* **68**, 850–858.

Thatcher, B. J., Doherty, A. E., Orvisky, E., Martin, B. M. & Henkin, R. I. (1998). *Biochem. Biophys. Res. Commun.* **250**, 635–641.

Vagin, A. & Teplyakov, A. (1997). *J. Appl. Cryst.* **30**, 1022–1025.

Youssef, R., Malaisse, W. J., Courtois, P. & Sener, A. (2003). *Int. J. Mol. Med.* **12**, 199–200.